AGU100 ADVANCING EARTH AND SPACE SCIENCE

Geophysical Research Letters

RESEARCH LETTER

10.1029/2018GL079678

Key Points:
- We present the first catchment-scale study of supraglacial pond energy balance, using seasonal pond coverages and 5,000 parameter sets
- Ponds cover 1.0% of debris-covered area (0.3% of total glacier area), yet energy receipts equate to 12.5 ± 2.0% of catchment annual mass loss
- Daily net surface energy balance was positive for the entire study period and elevation range, leading to a melt enhancement factor of 14 ± 3

Supporting Information:
- Supporting Information S1

Correspondence to:
E. S. Miles,
e.s.miles@leeds.ac.uk

Citation:
Miles, E. S., Willis, I., Buri, P., Steiner, J. F., Arnold, N. S., & Pellicciotti, F. (2018). Surface pond energy absorption across four Himalayan glaciers accounts for 1/8 of total catchment ice loss. *Geophysical Research Letters*, *45*, 10,464–10,473. https://doi.org/10.1029/2018GL079678

Received 18 JUL 2018
Accepted 10 SEP 2018
Accepted article online 17 SEP 2018
Published online 7 OCT 2018

Surface Pond Energy Absorption Across Four Himalayan Glaciers Accounts for 1/8 of Total Catchment Ice Loss

Evan S. Miles[1,2,3], Ian Willis[2], Pascal Buri[4], Jakob F. Steiner[5], Neil S. Arnold[2], and Francesca Pellicciotti[3,6]

[1]School of Geography, University of Leeds, Leeds, UK, [2]Scott Polar Research Institute, University of Cambridge, Cambridge, UK, [3]Mountain Hydrology and Mass Movements, Swiss Federal Institute for Forest, Snow and Landscape Research WSL, Birmensdorf, Switzerland, [4]Geophysical Institute, University of Alaska Fairbanks, Fairbanks, AK, USA, [5]Department of Geography, University of Utrecht, Utrecht, Netherlands, [6]Department of Geography, Northumbria University, Newcastle upon Tyne, UK

Abstract Glaciers in High Mountain Asia, many of which exhibit surface debris, contain the largest volume of ice outside of the polar regions. Many contain supraglacial pond networks that enhance melt rates locally, but no large-scale assessment of their impact on melt rates exists. Here we use surface energy balance modeling forced using locally measured meteorological data and monthly satellite-derived pond distributions to estimate the total melt enhancement for the four main glaciers within the 400-km^2 Langtang catchment, Nepal, for a 6-month period in 2014. Ponds account for 0.20 ± 0.03 m/year of surface melt, representing a local melt enhancement of a factor of 14 ± 3 compared with the debris-covered area, and equivalent to 12.5 ± 2.0% of total catchment ice loss. Given the prevalence of supraglacial ponds across the region, our results suggest that effective incorporation of melt enhancement by ponds is essential for accurate predictions of future mass balance change in the region.

Plain Language Summary Glaciers in the high mountains of Asia provide an important water resource for millions of people. Many of these glaciers are partially covered by rocky debris, which protects the ice from solar radiation and warm air. However, studies have found that the surface of these debris-covered glaciers is actually lowering as fast as glaciers without debris. Water ponded on the surface of the glaciers may be partially responsible, as water can absorb atmospheric energy very efficiently. However, the overall effect of these ponds has not been thoroughly assessed yet. We study a valley in Nepal for which we have extensive weather measurements, and we use a numerical model to calculate the energy absorbed by ponds on the surface of the glaciers over 6 months. As we have not observed each individual pond thoroughly, we run the model 5,000 times with different setups. We find that ponds are extremely important for glacier melt and absorb energy 14 times as quickly as the debris-covered ice. Although the ponds account for 1% of the glacier area covered by rocks, and only 0.3% of the total glacier area, they absorb enough energy to account for one eighth of the whole valley's ice loss.

1. Introduction

The glaciers in High Mountain Asia contain ~15,000 km^3 of ice, the largest reservoir outside of the polar regions (Grinsted, 2013) and play a crucial role in generating and regulating river discharges necessary for hydropower, irrigation, and sanitation for millions of people (Bolch et al., 2012; Immerzeel & Bierkens, 2012). The region's glaciers vary in surface characteristics, climatic setting, and sensitivity to climate change (Sakai & Fujita, 2017), but the majority of large valley glaciers exhibit a thick debris mantle over their ablation areas. Thick debris reduces surface melt (e.g., Östrem, 1959; Nicholson & Benn, 2012) and alters the glaciers' dynamic response to climate warming (e.g., Anderson & Anderson, 2016; Scherler et al., 2011). Despite the general ablation-reducing effect of thick surface debris, large-scale studies have identified comparable rates of thinning between debris-covered and debris-free glaciers in High Mountain Asia (Brun et al., 2017; Gardelle et al., 2013; Kääb et al., 2012).

Translating thinning rates into rates of melt for debris-mantled and debris-free areas is difficult due to differences in (1) glacier hypsometry and consequent meteorological setting (e.g., Ragettli et al., 2016; Vincent et al., 2016) and (2) glacier geometry and consequent flux divergence (Banerjee, 2017; Brun et al., 2018;

10.1029/2018GL079678

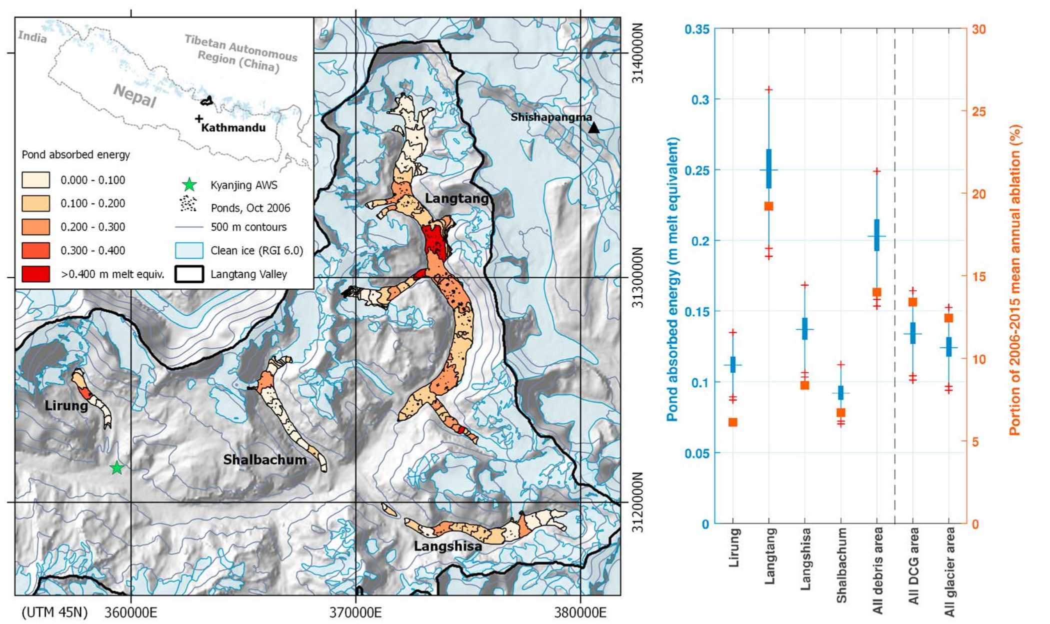

Figure 1. Location of the Langtang Valley in Nepal (inset), and principal glaciers in the valley, displaying median results for the cumulative April-October surface energy balance of supraglacial ponds in each 50-m elevation band, expressed as equivalent meters of surface melt in that band (left). Cumulative surface energy balance results for all 5,000 parameter sets are shown for each glacier as equivalent surface melt and as a portion of the mean annual 2006–2015 net ablation (right). *All debris area* refers to the equivalent thinning if spread over the glaciers' debris area, *All DCG area* instead uses the total glacier area for all glaciers that exhibit debris-covered tongues, and *All glacier area* corresponds to all glaciers in the catchment regardless of debris cover. Glacier outlines are updated from the RGI 6.0 (Pfeffer et al., 2014) as in Ragettli et al. (2016). RGI = Randolph Glacier Inventory.

Nuimura et al., 2017). Recent research has highlighted the role of supraglacial ponds and ice cliffs as areas of enhanced surface melt (e.g., Immerzeel, Kraaijenbrink, et al., 2014; Pellicciotti et al., 2015; Salerno et al., 2017), partially compensating for the reduced ablation over the debris-mantled areas. The spatial variability of these features leads to a heterogeneous pattern of surface ablation and drives a feedback of glacier surface evolution facilitating the development of new ponds and cliffs (Benn et al., 2012).

Melt rates at ice cliffs have been measured using photogrammetric and geodetic methods (Immerzeel, Kraaijenbrink, et al., 2014; Brun et al., 2016; Thompson et al., 2016; Watson, Quincey, Carrivick, et al., 2017) and have been modeled with increasing complexity (Buri, Miles, et al., 2016; Buri, Pellicciotti, et al., 2016; Han et al., 2010; Reid & Brock, 2014; Sakai et al., 1998, 2002). The effects of supraglacial ponds on ablation are more difficult to measure directly or model, but like ice cliffs, they also lead to local enhanced surface lowering for debris-covered glaciers (Benn et al., 2001; Miles et al., 2016; Röhl, 2006; 2008; Sakai et al., 2000; Salerno et al., 2017; Watson, Quincey, Smith, et al., 2017).

Ponds represent localized surface drainage inefficiency in the linked supraglacial/englacial drainage network of debris-covered glaciers, and fill and drain seasonally, moderating glacier discharge (Benn et al., 2012, 2017; Irvine-Fynn et al., 2017; Liu et al., 2015; Miles, Steiner, et al., 2017; Miles, Willis, et al., 2017; Narama et al., 2017). Due to their strongly positive surface energy balance, ponds warm seasonally and contribute to local surface ablation (Benn et al., 2001). Additionally, some atmospheric energy absorbed by ponds is delivered englacially via pond drainage to drive internal ablation along conduits (Benn et al., 2012; Sakai et al., 2000). The remaining melt energy is often dissipated through the postmonsoon and winter, although some ponds do maintain a winter heat reservoir (Watson et al., 2017; Xin et al., 2011). Thus, ponds can lead to considerable surface and internal ablation; although this has been evaluated for individual ponds on a few glaciers, it remains to be quantified at the glacier and catchment scales.

In this study we aim to provide the first glacier- and catchment-scale estimates of supraglacial pond surface energy balance and potential ablation for Himalayan debris-covered glaciers. This is achieved by leveraging unique data sets of supraglacial pond seasonality and near-surface meteorology in the Langtang catchment of Nepal to drive a supraglacial pond energy-balance model.

10.1029/2018GL079678

Table 1
Characteristics of the Debris-Covered Glaciers in the Langtang Valley and Cumulative Surface Energy Balance for Supraglacial Ponds in 2014

	Area (km^2)		Elevation (m a.s.l.)		Pond density	Thinning	Emergence	Pond April–October surface energy balance			*EF*
Glacier	Glacier	Debris	Min	Mean	% Debris area	(m/year)	(m/year)	$m^3 \times 10^5$ Ice	DCA m lowering	% DCA ablation	—
Shalbachum	11.7	2.8	4,218	4,607	0.7%	1.30 ± 0.20	0.07 ± 0.02	2.6 ± 0.4	0.09 ± 0.01	6.6% ± 1.4%	9 ± 2
Lirung	6.1	1.2	4,025	4,287	0.6%	1.67 ± 0.59	0.16 ± 0.1	1.4 ± 0.2	0.11 ± 0.02	6.0% ± 0.2%	10 ± 4
Langtang	52.8	17.8	4,468	4,944	1.3%	0.91 ± 0.05	0.39 ± 0.04	44.0 ± 7.0	0.25 ± 0.04	19.2% ± 3.2%	15 ± 2
Langshisa	21.7	4.4	4,526	4,884	0.5%	1.16 ± 0.23	0.48 ± 0.09	6.0 ± 1.0	0.14 ± 0.02	8.5% ± 1.9%	17 ± 4
All debris		26.2	4,025	4,906	1.0%	1.02 ± 0.18	0.43 ± 0.06	54.5 ± 8.6	0.20 ± 0.03	13.8% ± 2.9%	14 ± 3

Note. Minimum and mean elevation are for the DCA of each glacier. Pond density is the April–October mean pond coverage as a percent of the DCA (Miles, Willis, et al., 2017). Thinning is the mean observed lowering rate for each glacier's debris-covered area for 2006–2015 (Ragettli et al., 2016). Emergence is the mean emergence velocity over the entire DCA derived from flux gate calculations (supporting information). The ponds' cumulative surface energy balance is expressed as the volume equivalent if all energy was used to melt ice, as a mean ice melt rate for the glacier's DCA and as a fraction of the ablation (combination of thinning and emergence, all here in meters per year) in this area. *EF* is the melt enhancement factor for ponds relative to all other surface types (equation (1)). For all calculations $\rho_i = 900$ kg/m^3, and we show our results as $\mu \pm 2\sigma$ for the 5,000 model runs. DCA = debris-covered area.

2. Methods

We estimate the net surface energy balance of all supraglacial ponds for a typical ablation season within a large glacierized Himalayan catchment, the 400-km^2 Langtang catchment (Figure 1), which contains four valley glaciers varying in size, elevation, and debris cover. We use extensive local meteorological measurements and Landsat-derived monthly distributions of supraglacial ponds to drive a pond surface energy balance model (Miles et al., 2016) and use a Monte Carlo approach to account for uncertainty in key model parameters.

The study period is 15 April to 15 October 2014, the period when pond surfaces are most commonly thawed and for which local meteorological data are available. Meteorological observations were made at an automatic weather station located in nearby Kyanjing village for January–October 2014 (Figure 1), and we leverage an in-depth understanding of near-surface meteorology in the catchment based on a dense network of additional stations (Heynen et al., 2016; Immerzeel et al., 2014; Shea et al., 2015; Steiner & Pellicciotti, 2016). Based on these observations we transfer the meteorology observed at the automatic weather station to pond locations (see supporting information).

The study glaciers were partitioned into 50-m elevation bins according to a void-filled Shuttle Radar Topography Mission digital elevation model (Jarvis et al., 2008), and each glacier's monthly ponded area in each bin was prescribed based on Landsat TM/ETM+ pond measurements for 1999–2013 (Miles, Willis, et al., 2017). For each bin of each glacier, the mean monthly pond area from the Landsat archive was assumed to represent conditions in the middle of each month for 2014, and these were then linearly interpolated to hourly values for the 15 April to 15 October study period, producing a time series of pond surface area distributed along each glacier's elevation range.

The pond surface energy balance model of Miles et al. (2016) is applied to each 50-m elevation band across each glacier's debris-covered area. A full model description is available in supporting information. The model adjusts observations of incident radiation based on the ponds' topographic setting (Buri, Pellicciotti, et al., 2016; Ridley et al., 2010) and uses the bulk aerodynamic method with a stability correction to model turbulent fluxes. We employ a Monte Carlo approach to account for uncertainty in parameters that are difficult to constrain: albedo, emissivity, roughness length, and temperature of the water surface, as well as topographic view factors for each pond location. We construct 5,000 independent sets for these parameters, varying them randomly within their likely ranges (see supporting information; Brewster, 1992; Chikita & Joshi, 2000; Divine et al., 2015; Hicks, 1972; Jin et al., 2011; Katsaros et al., 1985; Sakai et al., 2009; Yamada, 1998; Yu et al., 2010) and calculate the energy balance for the entire catchment using each parameter set. We additionally test the sensitivity of the model to a $\pm$10% change in temperature lapse rates, as well as an empirical correction for on-glacier wind speeds.

For each glacier, and for the basin as a whole, we consider the cumulative pond surface energy balance as the ponds' *ablation potential* (Figure 1). To convert this ablation potential into portions of mass loss, we calculate the mean emergence velocity for each glacier's debris-covered area using a flux gate approach (supporting information; Cuffey & Paterson, 2010; Huss et al., 2007; Tadono et al., 2014; Vincent et al., 2016). These calculations are based on Glabtop2 ice thickness estimates (Frey et al., 2014) and high-confidence velocity fields derived from 2015 and 2016 RapidEye orthoimages using ImGraft (Dehecq et al., 2015; Messerli & Grinsted, 2015; Planet Team, 2017). We use the mean emergence velocity values to convert thinning rates observed by Ragettli et al. (2016) for the 2006–2015 period into mean annual ablation rates (Table 1). These calculations assume that pond coverage in 2014 was similar to the average coverage throughout 1999–2013, that the 2015–2016 annual velocity data set is similar to 1999–2013, and that ablation in 2014 was similar to the mean in the period 2006–2015. Consequently, these values represent long-term averages of the portion of thinning that could be attributable to pond-associated ablation rather than corresponding to a specific year. In addition, the calculations assume that all energy absorbed by supraglacial ponds leads to glacier melt; in this sense it is an upper bound on the role of supraglacial ponds. In reality, energy left in persistent ponds that do not drain during the monsoon will instead dissipate over winter, while other ponds may drain rapidly and advect unused energy out of the glacier.

Based on the modeled ablation potential, we calculate a pond-associated ablation enhancement factor (*EF*) for each glacier and for the entire study area as the ratio of the rate of pond energy absorption to average

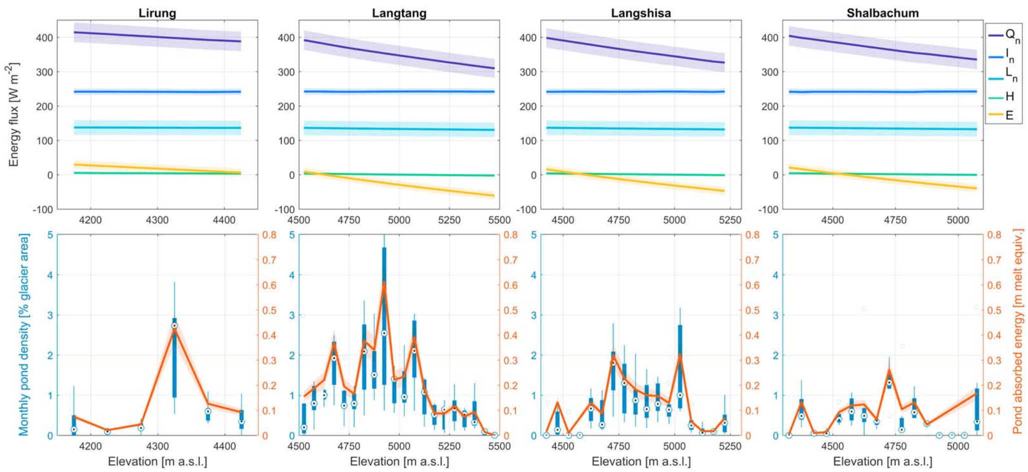

Figure 2. Pond surface energy balance results show a slight decay in Q_n for the altitudinal range of each glacier (top). Ponded area shows considerable variability between glaciers and with elevation. Ponds could account for up to 0.5 m of ablation for individual elevation bands (bottom).

ablation rates for the entire debris-covered area,

$$EF = \frac{M_p/\overline{A_p}}{\bar{\dot{h}} + \overline{w_e}}, \tag{1}$$

where M_p is the atmospheric energy absorbed by ponds annually (m^3/a ice melt), $\overline{A_p}$ is the mean ponded area (m^2), $\bar{\dot{h}}$ is the mean annual surface lowering (m/year; Ragettli et al., 2016), and $\overline{w_e}$ is the mean emergence velocity (m/year; see supporting information), both for the debris-covered area.

3. Results

3.1. Overall Pond Energy Absorption

We find that ponds are a major avenue of atmospheric melt energy for debris-covered glaciers. Across the catchment, pond-absorbed energy equates to 0.20 $\pm$ 0.02 m (expressed here and after as $\mu \pm 2\sigma$) melt over the entire debris-covered area, accounting for 13.8 $\pm$ 2.9% of the annual ablation for the entire debris-covered area. Ponds thus could account for 12.5 $\pm$ 2.0% of net annual mass loss for the total glacierized area in the valley including mass loss for entirely debris-free glaciers.

Supraglacial pond energy absorption varies between glaciers by several orders of magnitude depending on each glacier's size, hypsometry, and monthly pond densities (Table 1). The whole-valley energy absorption is dominated by Langtang Glacier's ponds, which absorbed enough energy to melt 4.4 $\times$ 10^6 m^3 of ice over the 6-month study period, equivalent to 0.25 $\pm$ 0.04 m of surface melt if distributed across the glacier's debris-covered area. Compared to the 2006–2015 observed thinning, corrected for mean emergence velocity, Langtang Glacier's ponds are responsible for 19.2 $\pm$ 3.2% of the net ablation across its debris-covered area (Table 1). Ponds account for 6–9% of the net ablation for the three other major debris-covered glaciers.

Pond melt enhancement factors also vary between glaciers, ranging from 9 $\pm$ 2 for Shalbachum Glacier to 17 $\pm$ 3 for Langshisa Glacier (Table 1). Across the whole valley, ponds absorb energy at a rate of 14 $\pm$ 3 times that of the debris-covered area. Emergence velocity is a primary source of uncertainty in this calculation due to the regional scarcity of direct measurements of emergence or ice thickness.

3.2. Altitudinal and Seasonal Changes in Pond Energy Balance

Our results show a marked altitudinal decrease in mean April–October net pond surface energy balance (Figure 2). The primary driver of this altitudinal decrease is the latent turbulent heat flux, which decreases 100 W/m^2 between 4,150 and 5,400 m a.s.l., changing from an atmospheric source to a sink of energy at ~4,550 m. The sensible turbulent heat flux also shows a moderate decrease with altitude but remains low in magnitude. These reductions with altitude are due primarily to the air temperature lapse rates, which control water surface temperatures. Shortwave and longwave radiative fluxes do not vary significantly with altitude as their topographic controls are modeled stochastically. Despite the latent energy sink at higher elevations,

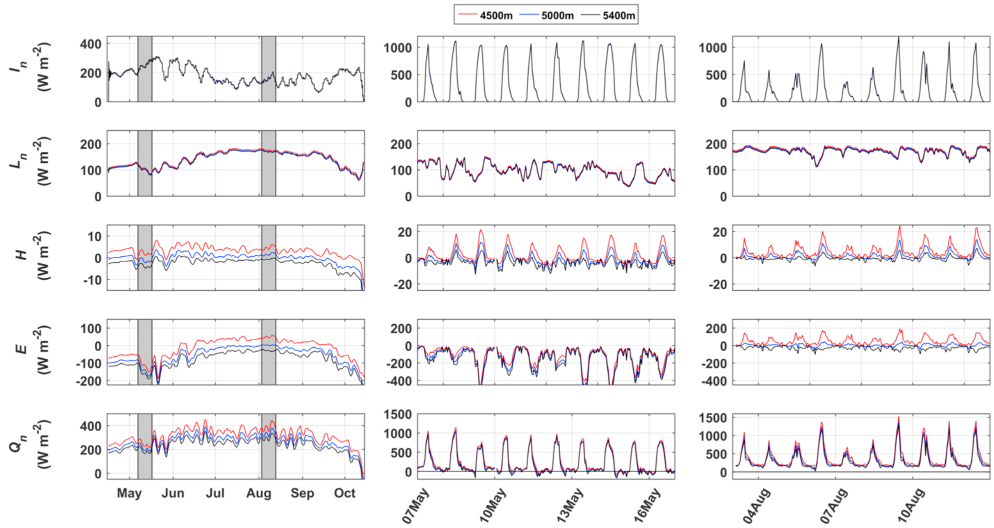

Figure 3. Daily mean surface energy balance components at 4,500, 5,000, and 5,400 m at Langtang Glacier for the full study period from our median model run (left). Shaded boxes correspond to the periods from May (middle) and August (right) showing hourly results, highlighting the difference in diurnal energy fluxes between the premonsoon and monsoon. Energy fluxes shown are shortwave balance I_n (top row, with lower altitude results plotted beneath the 5,400-m data set), longwave balance L_n, sensible (H), and latent (E) turbulent fluxes, and the net surface energy balance Q_n. Note differing y-axis scales for clarity.

the net surface energy balance is strongly positive for the entire modeled elevation range. Consequently, high-altitude ponds can remain thawed and absorb energy even when mean daily air temperatures are below freezing (above 5,150 m for our study period in the Langtang Valley), suggesting high-altitude ponds still act as seasonal recipients of atmospheric energy.

The pond surface energy balance is strongly affected by seasonal variations in meteorological conditions associated with the South Indian Monsoon. We find that seasonal differences in pond surface energy fluxes are of a greater magnitude than the altitudinal variations, and the daily mean net surface energy balance remains positive at all elevations for the entire study period (Figure 3). Monsoon-driven decreases in net shortwave radiation due to cloud cover are overcome by increases in net longwave radiation and latent heat fluxes due to warming air temperatures. Diurnal fluctuations are common for all surface energy fluxes, but they vary distinctly with elevation and between the premonsoon and monsoon (Figure 3). Diurnal variations in net shortwave receipts are often reduced in the monsoon compared to the premonsoon due to cloud cover, whereas net longwave receipts increase in magnitude and decrease in diurnal variability due to higher temperatures and increased cloud cover. Little seasonal change is evident in the sensible fluxes, but between the premonsoon and the monsoon the latent fluxes greatly reduce in diurnal variability and, for lower elevations, switch from an energy sink to a source. The resulting net surface energy balance has negative nighttime values at all elevations in the premonsoon, indicating regular refreezing, but is always positive in the monsoon.

4. Discussion

4.1. Spatial Variations in Pond-Absorbed Energy

The extent of supraglacial ponding is the primary control on the magnitude of pond energy absorption, while altitudinal differences are of secondary importance (Figure 2). Consequently, glaciers with high pond density at lower altitudes are the strongest recipients of energy via ponds. This is the case across individual glaciers as well: Areas with greater pond concentration will be the most affected, as demonstrated by several elevation bands on Langtang Glacier that absorb melt-equivalent energy >0.2 m (maximum 0.47 m, Figure 1). Such energy absorbed by ponds will lead to local surface ablation while the ponds are present, and drive internal ablation down-glacier when ponds drain, leading to a variable, punctuated expression of surface lowering across the debris-covered areas of the glaciers reported here and Himalayan glaciers more generally (Immerzeel, Kraaijenbrink, et al., 2014; Thompson et al., 2016).

As pond extent is a primary control on overall glacier mass loss (Salerno et al., 2017), we assess the prevalence of ponding in this study relative to other debris-covered glaciers in order to consider the regional implications of our findings. The average concentration of supraglacial ponds in the debris-covered areas of the Langtang catchment ranges from 0.5% to 1.7%, with a mean of 1.0% (Table 1). This is within the range observed for other glaciers, such as in the Everest region, where pond densities vary from 0.2% to 6.3% (Watson et al., 2016). Considering the entire Hindu Kush Himalaya mountain range, Gardelle et al. (2011) found pond extent was highly variable, covering 0.01% to 0.4% of total glacier area (we find 0.3% for our domain). Thus, while the error for our Landsat-derived pond coverages is not insignificant (Miles, Willis, et al., 2017), our results are appropriate for the Central Himalaya, and there may be considerable variability in the overall role of ponds throughout the region.

4.2. Comparison to Other Studies and Limitations

Our results indicate that ponds absorb sufficient energy to account for an impressive 12.5 $\pm$ 2.0% of annual glacier mass loss in the Langtang catchment of Nepal despite covering only 1% of the catchment's debris-covered area, or 0.3% of the total glacier area. Our energy-balance approach is the most sophisticated yet to be applied to Himalayan supraglacial ponds and the only one to have been applied at the catchment scale, but three previous estimates of pond-associated ablation are useful for comparison. Sakai et al. (2000) attributed 3.4% of Lirung Glacier's total ablation to ponds although they covered only 0.43% of the debris-covered area, but they used a less sophisticated energy balance model. Focusing on the terminus area of the Tasman Glacier, Röhl (2008) attributed 10% of all ice loss to supraglacial ponds, although that study estimated only the effects of ponds at the glacier's surface (it did not estimate internal ablation), and Tasman Glacier has a very different meteorological setting compared to Himalayan glaciers. Thompson et al. (2016) estimated an upper bound of Ngozumpa Glacier's internal ablation of 9% based on the surface subsidence associated with submarginal conduits; this would account only for energy advected into the glacier by pond drainage.

Our energy-balance approach makes key advances over these previous studies in terms of formulation and scale of analysis. Nonetheless, many dynamic local processes affecting pond temperature could not be represented, such as natural or wind-driven pond overturning and losses of energy to proximal ice cliffs (Miles et al., 2016), as the model is built to suit application over glacier and catchment scales rather than individual ponds. We have attempted to account for input data limitations through a Monte Carlo approach with a wide range of parameter sets, and our results are very consistent ($\mu \pm 2\sigma = 12.5 \pm 2.0\%$ of the whole catchment ice loss). We have also tested the model's response to reduced or enhanced air temperature lapse rates; both lead to less than 10% change in the mean values from our 5,000 parameter sets (supporting information). The on-glacier wind correction has a more substantial effect (15% change in mean value) underlining the importance of locally representative meteorological forcing. Opportunities exist for future improvement of the model and its application; the model could be adapted to directly model local subaqueous melt, or to represent pond surface freeze-thaw cycles, which occur seasonally and diurnally at higher elevations. Additional measurements are needed to better prescribe some input data, especially for supraglacial pond albedo and surface temperature.

The lack of direct emergence velocity or ice thickness measurements for debris-covered glaciers makes it difficult to convert thinning rates to ablation over the debris-covered area. Emergence velocities are usually <0.5 m/year over the lower portion of the debris-covered area but can be considerable near the clean ice transition (Immerzeel, Kraaijenbrink, et al., 2014; Nuimura et al., 2017; Rounce et al., 2018; Vincent et al., 2016). Our flux gate method is useful for estimating the magnitude of emergence velocity but is dependent on ice thickness modeled using Glabtop2 (Frey et al., 2014). Glabtop2 performed reasonably well in the ice thickness model intercomparison experiment (Farinotti et al., 2017), with a mean bias of −34% for glaciers, but all models' performance varied greatly between glaciers. Consequently, direct measurements of ice thickness and emergence velocity are a high priority for the region.

4.3. Outlook for Modeling Pond Ablation at Large Scales

Our results show the potential for ponds to cause significant surface and internal ablation, which has rarely been represented in models of glacier mass balance and evolution. The 14% of net ablation for debris-covered glacier areas attributable to supraglacial ponds is in addition to the heightened ablation at ice cliffs, which account for an additional 23–24% of ablation for this area (e.g., Brun et al., 2018). Efforts to date have represented ponds and cliffs as areas of reduced debris thickness (Ragettli et al., 2015) or as areas with a constant melt enhancement factor (Kraaijenbrink et al., 2017, who used a factor of 10). These efforts are limited by the static representation of ponded area; although the use of an enhancement factor is a practical approach to include the first-order effects of pond-associated mass loss within large-scale models, such studies should consider a range of *EF* values to account for differences between glaciers and ensure they use seasonally representative pond distributions.

A more sophisticated approach, as in this study, could be applied across the entire region using downscaled regional climatology, but there is a need for representative seasonal pond coverage data sets for other catchments in the region. Supraglacial pond cover varies seasonally, but most assessments of supraglacial ponding have focused on the postmonsoon, when atmospheric stability leads to cloud-free imagery but when pond cover can be at its lowest due to seasonal drainage (Liu et al., 2015; Miles, Willis, et al., 2017; Müller, 1968; Narama et al., 2017). Moreover, surface ponds can be small and highly transient features, appearing and disappearing over periods of a few days to a few years, so such data sets must be of high resolution in both space and time (Benn et al., 2017; Miles et al., 2017; Watson et al., 2016).

5. Conclusions

We use surface energy balance modeling, forced by local meteorological data and monthly satellite-derived supraglacial pond distributions to estimate the total pond-associated ablation for four glaciers within the Langtang catchment of Nepal, for a 6-month period in 2014. Ponds enhance melt rates by a factor of 14 ± 3 compared with other surface types, and account for 0.20 ± 0.03 m/year of surface lowering, equivalent to $12.5 \pm 2.5\%$ of total catchment ice loss. This is the first assessment of the total impact of pond-generated ablation at the catchment scale.

Pond energy absorption will lead to ablation at the surface of the glaciers locally and inside the glaciers along conduits and has a strong spatial and seasonal variability forced by the glacier-specific spatiotemporal distribution of ponds. Pond energy absorption is also controlled by the seasonal variability in meteorological conditions and the altitudinal decrease of air temperature, but the mean daily pond surface energy balance remains strongly positive for the entire debris-covered area and for the entire study duration. Our results confirm supraglacial ponds as major contributors to mass loss for debris-covered glaciers in the Central Himalaya, not only responding to but also contributing to the decline in longitudinal gradient for heavily debris-covered glaciers. In addition to the need to better constrain the ablation due to supraglacial ice cliffs and the thickness of these glaciers, our study highlights the need for improved pond occurrence data sets measured at high spatial and temporal resolution in order to accurately assess the evolution of debris-covered glaciers in the 21st century.

Acknowledgments
Model results are archived and available at Zenodo (Miles et al., 2018). The authors gratefully acknowledge the USGS and NASA Land Processes Distributed Active Archive Center for free Landsat data access. ASTER is a product of METI and NASA. We thank Silvan Ragettli for provision of his thinning rates and Philip Kraaijenbrink for sharing his implementation of Glabtop2. We are thankful for the efforts of Walter Immerzeel, Joseph Shea, and the International Centre for Integrated Mountain Development to install and maintain an extensive meteorological network in the Langtang Valley. We also thank Tek Rai and his logistics team for field support during our own field work in Langtang. E. S. M. acknowledges financial support from the Gates Cambridge Trust, Trinity College (Cambridge), and the Philip Lake and William Vaughn Lewis Fund (Cambridge). I. C. W. and E. S. M. acknowledge fieldwork funding from the B.B. Roberts Fund (Cambridge). J. F. S. acknowledges support from the European Research Council under the European Union's Horizon 2020 research and innovation programme (grant agreement 676819). Fieldwork was also supported by the USAID (United States Agency for International Development) High Mountain Glacier Watershed Programs Climber-Scientist Grant (CCRDCS0010) and the Swiss National Science Foundation project UNCOMUN (SNF 200021L146761).

References

Anderson, L. S., & Anderson, R. S. (2016). Modeling debris-covered glaciers: Extension due to steady debris input. *The Cryosphere*, *10*, 1105–1124. https://doi.org/10.5194/tcd-9-6423-2015

Banerjee, A. (2017). Brief communication: Thinning of debris-covered and debris-free glaciers in a warming climate. *The Cryosphere*, *11*, 133–138. https://doi.org/10.5194/tc-2016-121

Benn, D., Bolch, T., Hands, K., Gulley, J., Luckman, A., Nicholson, L., et al. (2012). Response of debris-covered glaciers in the Mount Everest region to recent warming, and implications for outburst flood hazards. *Earth-Science Reviews*, *114*(1-2), 156–174. https://doi.org/10.1016/j.earscirev.2012.03.008

Benn, D. I., Thompson, S., Gulley, J., Mertes, J., Luckman, A., & Nicholson, L. (2017). Structure and evolution of the drainage system of a Himalayan debris- covered glacier, and its relationship with patterns of mass loss. *The Cryosphere*, *11*(March), 2247–2264. https://doi.org/10.5194/tc-11-2247-2017

Benn, D. I., Wiseman, S., & Hands, K. A. (2001). Growth and drainage of supraglacial lakes on debris-mantled Ngozumpa Glacier, Khumbu Himal, Nepal. *Journal of Glaciology*, *47*(159), 626–638. https://doi.org/10.3189/172756501781831729

Bolch, T., Kulkarni, A., Kaab, A., Huggel, C., Paul, F., Cogley, J. G., et al. (2012). The state and fate of Himalayan glaciers. *Science (New York, N.Y.)*, *306*(6079), 310–314. https://doi.org/10.1126/science.1215828

Brewster, M. Q. (1992). *Thermal Radiative Transfer and Properties*. New York: John Wiley & Sons.

Brun, F., Berthier, E., Wagnon, P., Kääb, A., & Treichler, D. (2017). A spatially resolved estimate of High Mountain Asia glacier mass balances, 2000-2016. *Nature Geoscience*, *10*, 668–673. https://doi.org/10.1038/ngeo2999

Brun, F., Buri, P., Miles, E. S., Wagnon, P., Steiner, J. F., Berthier, E., et al. (2016). Quantifying volume loss from ice cliffs on debris-covered glaciers using high resolution terrestrial and aerial photogrammetry. *Journal of Glaciology*, *62*(234), 684–695. https://doi.org/10.1017/jog.2016.54

Brun, F., Wagnon, P., Berthier, E., Shea, J. M., Immerzeel, W. W., Kraaijenbrink, D. A., et al. (2018). Can ice-cliffs explain the "debris-cover anomaly "? New insights from Changri Nup Glacier, Nepal, Central Himalaya. *The Cryosphere Discussions*, 1–32. https://doi.org/10.5194/tc-2018-38

Buri, P., Miles, E. S., Steiner, J. F., Immerzeel, W., Wagnon, P., Pellicciotti, F., et al. (2016). A physically-based 3D model of ice cliff evolution on a debris-covered glacier. *Journal of Geophysical Research: Earth Surface*, *121*, 2471–2493. https://doi.org/10.1002/2016JF004039

Buri, P., Pellicciotti, F., Steiner, J. F., Miles, E. S., & Immerzeel, W. W. (2016). A grid-based model of backwasting of supraglacial ice cliffs on debris-covered glaciers. *Annals of Glaciology*, *57*(71), 199–211. https://doi.org/10.3189/2016AoG71A059

Chikita, K., & Joshi, S. (2000). Hydrological and thermal regimes in a supra-glacial lake: Imja, Khumbu, Nepal Himalaya. *Hydrological Sciences*, *45*(4), 507–522.

Cuffey, K. M., & Paterson, W. (2010). *The Physics of Glaciers* (4th ed.). Oxford, UK: Elsevier B.V.

Dehecq, A., Gourmelen, N., & Trouve, E. (2015). Deriving large-scale glacier velocities from a complete satellite archive: Application to the Pamir âĂŞ Karakoram âĂŞ Himalaya. *Remote Sensing of Environment*, *162*, 55–66.

Divine, D. V., Granskog, M. A., Hudson, S. R., Pedersen, C. A., Karlsen, T. I., Divina, S. A., et al. (2015). Regional melt-pond fraction and albedo of thin Arctic first-year drift ice in late summer. *The Cryosphere*, *9*(1), 255–268. https://doi.org/10.5194/tc-9-255-2015

Farinotti, D., Brinkerhoff, D. J., Clarke, G. K. C., Fürst, J. J., Frey, H., Gantayat, P., et al. (2017). How accurate are estimates of glacier ice thickness? Results from ITMIX, the Ice Thickness Models Intercomparison eXperiment. *The Cryosphere*, *11*, 949–970. https://doi.org/10.5194/tc-11-949-2017

Frey, H., Machguth, H., Huss, M., Huggel, C., Bajracharya, S., Bolch, T., et al. (2014). Estimating the volume of glaciers in the Himalayan Karakoram region using different methods. *The Cryosphere*, *8*(6), 2313–2333. https://doi.org/10.5194/tc-8-2313-2014

Gardelle, J., Arnaud, Y., & Berthier, E. (2011). Contrasted evolution of glacial lakes along the Hindu Kush Himalaya mountain range between 1990 and 2009. *Global and Planetary Change*, *75*(1-2), 47–55. https://doi.org/10.1016/j.gloplacha.2010.10.003

Gardelle, J., Berthier, E., Arnaud, Y., & Kääb, A. (2013). Region-wide glacier mass balances over the Pamir-Karakoram-Himalaya during 1999-2011. *The Cryosphere*, *7*(4), 1263–1286. https://doi.org/10.5194/tc-7-1263-2013

Grinsted, A. (2013). An estimate of global glacier volume. *The Cryosphere*, *7*(1), 141–151. https://doi.org/10.5194/tc-7-141-2013

Han, H., Wang, J., Wei, J., & Liu, S. (2010). Backwasting rate on debris-covered Koxkar glacier, Tuomuer mountain, China. *Journal of Glaciology*, *56*(196), 287–296. https://doi.org/10.3189/002214310791968430

Heynen, M., Miles, E., Ragettli, S., Buri, P., Immerzeel, W., & Pellicciotti, F. (2016). Air temperature variability in a high elevation Himalayan catchment. *Annals of Glaciology*, *57*(71), 212–222. https://doi.org/10.3189/2016AoG71A076

Hicks, B. B. (1972). Some evaluations of drag and bulk transfer coefficients over water bodies of different sizes. *Boundary-Layer Meteorology*, *3*(2), 201–213. https://doi.org/10.1007/BF02033919

Huss, M., Sugiyama, S., Bauder, A., Funk, M., Huss, M., Bauder, A., et al. (2007). Retreat scenarios of Unteraargletscher, Switzerland, using a combined ice-flow mass-balance model retreat scenarios of Unteraargletscher, Switzerland, using a combined ice-flow mass-balance model, Arctic, Antarctic and Alpine Research vol. 39, 3, https://doi.org/10.1657/1523-0430(06-036)

Immerzeel, W. W., & Bierkens, M. F. P. (2012). Asia's water balance. *Nature Geoscience*, *5*(12), 841–842. https://doi.org/10.1038/ngeo1643

Immerzeel, W., Kraaijenbrink, P., Shea, J., Shrestha, A., Pellicciotti, F., Bierkens, M., et al. (2014). High-resolution monitoring of Himalayan glacier dynamics using unmanned aerial vehicles. *Remote Sensing of Environment*, *150*, 93–103. https://doi.org/10.1016/j.rse.2014.04.025

Immerzeel, W. W., Petersen, L., Ragettli, S., & Pellicciotti, F. (2014). The importance of observed gradients of air temperature and precipitation for modeling runoff from a glacierized watershed in the Nepalese Himalayas. *Water Resources Research*, *50*, 2212–2226. https://doi.org/10.1002/2013WR014506

Irvine-Fynn, T. D., Porter, P. R., Rowan, A. V., Quincey, D. J., Gibson, M. J., Bridge, J. W., et al. (2017). Supraglacial ponds regulate runoff from Himalayan debris-covered glaciers. *Geophysical Research Letters*, *44*, 11,894–11,904. https://doi.org/10.1002/2017GL075398

Jarvis, A., Reuter, H., Nelson, A., & Guevara, E. (2008). Hole-filled SRTM for the globe Version 4, available from the CGIAR-CSI SRTM 90Database (http:/srtm.csi.cgiar.org).

Jin, Z., Qiao, Y., Wang, Y., Fang, Y., & Yi, W. (2011). A new parameterization of spectral and broadband ocean surface albedo. *Optics Express*, *19*(27), 6493–6499. https://doi.org/10.1029/96JC00629.K

Kääb, A., Berthier, E., Nuth, C., Gardelle, J., & Arnaud, Y. (2012). Contrasting patterns of early twenty-first-century glacier mass change in the Himalayas. *Nature*, *488*(7412), 495–498. https://doi.org/10.1038/nature11324

Katsaros, K. B., McMurdie, L. a., Lind, R. J., & DeVault, J. E. (1985). Albedo of a water surface, spectral variation, effects of atmospheric transmittance, sun angle and wind speed. *Journal of Geophysical Research*, *90*(5), 7313. https://doi.org/10.1029/JC090iC04p07313

Kraaijenbrink, P. D., Bierkens, M. F., Lutz, A. F., & Immerzeel, W. W. (2017). Impact of a global temperature rise of 1.5 degrees Celsius on Asia's glaciers. *Nature*, *549*(7671), 257–260. https://doi.org/10.1038/nature23878

Liu, Q., Mayer, C., & Liu, S. (2015). Distribution and interannual variability of supraglacial lakes on debris-covered glaciers in the Khan Tengri-Tomur Mountains, Central Asia. *Environmental Research Letters*, *10*, 4545–4584. https://doi.org/10.1088/1748-9326/10/1/014014

Messerli, A., & Grinsted, A. (2015). Image georectification and feature tracking toolbox: ImGRAFT, Geoscientific Instrumentation. *Methods and Data Systems*, *4*(1), 23–34. https://doi.org/10.5194/gi-4-23-2015

Miles, E. S., Pellicciotti, F., Willis, I. C., Steiner, J. F., Buri, P., & Arnold, N. S. (2016). Refined energy-balance modelling of a supraglacial pond, Langtang Khola, Nepal. *Annals of Glaciology*, *57*(71), 29–40. https://doi.org/10.3189/2016AoG71A421

Miles, E. S., Steiner, J., Willis, I. C., Buri, P., Immerzeel, W. W., Chesnokova, A., et al. (2017). Pond dynamics and supraglacial-englacial connectivity on debris-covered Lirung Glacier, Nepal. *Frontiers in Earth Science*, *5*(69), 1–19. https://doi.org/10.3389/FEART.2017.00069

Miles, E. S., Willis, I. C., Arnold, N. S., Steiner, J. F., & Pellicciotti, F. (2017). Spatial, seasonal, and interannual variability of supraglacial ponds in the Langtang Valley of Nepal, 1999 to 2013. *Journal of Glaciology*, *63*(237), 88–105. https://doi.org/10.1017/jog.2016.120

Miles, E. S., Willis, I. C., Buri, P., Steiner, J. F., Arnold, N. S., & Pellicciotti, F. (2018). Model results for 'Surface pond energy absorption across four Himalayan glaciers accounts for 1/8 of total catchment ice loss', Zenodo https://doi.org/10.5281/zenodo.1344919

Müller, F. (1968). Mittelfristige Schwankungen der Oberflächengeschwindigkeit des Khumbugletschers am Mount Everest. *Schweizerische Bauzeitung*, *86*(31), 569–573. https://doi.org/10.5169/seals-70102

Narama, C., Daiyrov, M., Tadono, T., Yamamoto, M., Kääb, A., Morita, R., et al. (2017). Seasonal drainage of supraglacial lakes on debris-covered glaciers in the Tien Shan Mountains, Central Asia. *Geomorphology*, *286*, 133–142. https://doi.org/10.1016/j.geomorph.2017.03.002

Nicholson, L., & Benn, D. I. (2012). Properties of natural supraglacial debris in relation to modelling sub-debris ice ablation. *Earth Surface Processes and Landforms*, *38*(5), 490–501. https://doi.org/10.1002/esp.3299

Nuimura, T., Fujita, K., & Sakai, A. (2017). Downwasting of the debris-covered area of Lirung Glacier in Langtang Valley, Nepal Himalaya, from 1974 to 2010. *Quaternary International*, *455*, 93–101. https://doi.org/10.1016/j.quaint.2017.06.066

Östrem, G. (1959). Ice melting under a thin layer of moraine, and the existence of ice cores in moraine ridges. *Geografiska Annaler*, *41*(4), 228–230.

Pellicciotti, F., Stephan, C., Miles, E., Herreid, S., Immerzeel, W. W., & Bolch, T. (2015). Mass-balance changes of the debris-covered glaciers in the Langtang Himal, Nepal, 1974–99. *Journal of Glaciology*, *61*(226), 1–14. https://doi.org/10.3189/2015JoG13J237

Pfeffer, W. T., Arendt, A. a., Bliss, A., Bolch, T., Cogley, J. G., Gardner, A. S., et al. (2014). The Randolph Glacier Inventory: A globally complete inventory of glaciers, The Randolph Consortium. *Journal of Glaciology*, *60*(221), 537–552. https://doi.org/10.3189/2014JoG13J176

Planet Team (2017). Planet application program interface: In space for life on Earth.

Ragettli, S., Bolch, T., & Pellicciotti, F. (2016). Heterogeneous glacier thinning patterns over the last 40 years in Langtang Himal. *The Cryosphere*, *10*(5), 2075–2097. https://doi.org/10.5194/tc-10-2075-2016

Ragettli, S., Pellicciotti, F., Immerzeel, W. W., Miles, E. S., Petersen, L., Heynen, M., et al. (2015). Unraveling the hydrology of a Himalayan catchment through integration of high resolution in situ data and remote sensing with an advanced simulation model. *Advances in Water Resources*, *78*, 94–111. https://doi.org/10.1016/j.advwatres.2015.01.013

Reid, T., & Brock, B. (2014). Assessing ice-cliff backwasting and its contribution to total ablation of debris-covered Miage glacier, Mont Blanc massif, Italy. *Journal of Glaciology*, *60*(219), 3–13. https://doi.org/10.3189/2014JoG13J045

Ridley, B., Boland, J., & Lauret, P. (2010). Modelling of diffuse solar fraction with multiple predictors. *Renewable Energy*, *35*(2), 478–483. https://doi.org/10.1016/j.renene.2009.07.018

Röhl, K. (2006). Thermo-erosional notch development at fresh-water-calving Tasman Glacier, New Zealand. *Journal of Glaciology*, *52*(177), 203–213.

Röhl, K. (2008). Characteristics and evolution of supraglacial ponds on debris-covered Tasman Glacier, New Zealand. *Journal of Glaciology*, *54*(188), 867–880. https://doi.org/10.3189/002214308787779861

Rounce, D. R., King, O., McCarthy, M., Shean, D. E., & Salerno, F. (2018). Quantifying debris thickness of debris-covered glaciers in the Everest Region of Nepal through inversion of a subdebris melt model. *Journal of Geophysical Research: Earth Surface*, *123*, 1094–1115. https://doi.org/10.1029/2017JF004395

Sakai, A., & Fujita, K. (2017). Contrasting glacier responses to recent climate change in high-mountain Asia. *Scientific Reports*, *7*, 13717. https://doi.org/10.1038/s41598-017-14256-5

Sakai, A., Nakawo, M., & Fujita, K. (1998). Melt rate of ice cliffs on the Lirung Glacier, Nepal Himalayas, 1996. *Bulletin of Glacier Research*, *16*, 57–66.

Sakai, A., Nakawo, M., & Fujita, K. (2002). Distribution characteristics and energy balance of ice cliffs on debris-covered glaciers, Nepal Himalaya, Arctic. *Antarctic, and Alpine Research*, *34*(1), 12. https://doi.org/10.2307/1552503

Sakai, A., Nishimura, K., Kadota, T., & Takeuchi, N. (2009). Onset of calving at supraglacial lakes on debris-covered glaciers of the Nepal Himalaya. *Journal of Glaciology*, *55*(193), 909–917. https://doi.org/10.3189/002214309790152555

Sakai, A., Takeuchi, N., Fujita, K., & Nakawo, M. (2000). Role of supraglacial ponds in the ablation process of a debris-covered glacier in the Nepal Himalayas. *Debris-Covered Glaciers*, *264*, 119–130.

Salerno, F., Thakuri, S., Fujita, K., & Nuimura, T. (2017). Debris-covered glacier anomaly? Morphological factors controlling changes in mass balance, surface area, terminus position, and snow line altitude of Himalayan glaciers. *Earth and Planetary Science Letters*, *471*, 19–31. https://doi.org/10.1016/j.epsl.2017.04.039

Scherler, D., Bookhagen, B., & Strecker, M. R. (2011). Spatially variable response of Himalayan glaciers to climate change affected by debris cover. *Nature Geoscience*, *4*(3), 156–159. https://doi.org/10.1038/ngeo1068

Shea, J. M., Wagnon, P., Immerzeel, W. W., Biron, R., Brun, F., & Pellicciotti, F. (2015). A comparative high-altitude meteorological analysis from three catchments in the Nepalese Himalaya. *International Journal of Water Resources Development*, *31*(2), 174–200. https://doi.org/10.1080/07900627.2015.1020417

Steiner, J., & Pellicciotti, F. (2016). On the variability of air temperature over a debris covered glacier, Nepalese Himalaya. *Annals of Glaciology*, *57*(71), 295–307.

Tadono, T., Ishida, H., Oda, F., Naito, S., Minakawa, K., & Iwamoto, H. (2014). Precise global DEM generation by ALOS PRISM. In *ISPRS Annals of Photogrammetry, Remote Sensing and Spatial Information Sciences Technical Commission IV Symposium (Vol. II-4)* pp. 14–16. https://doi.org/10.5194/isprsannals-II-4-71-2014

Thompson, S., Benn, D. I., Mertes, J., & Luckman, A. (2016). Stagnation and mass loss on a Himalayan debris-covered glacier: Processes, patterns and rates. *Journal of Glaciology*, *62*, 467–485. https://doi.org/10.1017/jog.2016.37

Vincent, C., Wagnon, P., Shea, J. M., Immerzel, W. W., Kraaijenbrink, P. D. A., Shrestha, D., et al. (2016). Reduced melt on debris-covered glaciers: Investigations from Changri Nup Glacier, Nepal. *The Cryosphere*, *10*, 1845–1858. https://doi.org/10.5194/tc-10-1845-2016

Watson, C. S., Quincey, D. J., Carrivick, J. L., & Smith, M. W. (2016). The dynamics of supraglacial ponds in the Everest region, central Himalaya. *Global and Planetary Change*, *142*, 14–27. https://doi.org/10.1016/j.gloplacha.2016.04.008

Watson, C. S., Quincey, D. J., Carrivick, J. L., Smith, M. W., Rowan, A. V., & Richardson, R. (2017). Heterogeneous water storage and thermal regime of supraglacial ponds on debris-covered glaciers. *Earth Surface Processes and Landforms*, *43*, 229–241. https://doi.org/10.1002/esp.4236

Watson, C. S., Quincey, D. J., Smith, M. W., Carrivick, J. L., Rowan, A. V., & James, M. R. (2017). Quantifying ice cliff evolution with multi-temporal point clouds on the debris-covered Khumbu Glacier, Nepal. *Journal of Glaciology*, *63*(241), 823–837. https://doi.org/10.1017/jog.2017.47

Xin, W., Shiyin, L., Han, H., Jian, W., & Qiao, L. (2011). Thermal regime of a supraglacial lake on the debris-covered Koxkar Glacier, southwest Tianshan, China. *Environmental Earth Sciences*, *67*(1), 175–183. https://doi.org/10.1007/s12665-011-1490-1

Yamada, T (1998). Glacier lake and its outburst flood in the Nepal Himalaya.

Yu, Y., Chen, H., Xia, X., Xuan, Y., & Yu, K. (2010). Significant variations of surface albedo during a snowy period at Xianghe observatory, China. *Advances in Atmospheric Sciences*, *27*(1), 80–86. https://doi.org/10.1007/s00376-009-8151-2